Clinical and Translational Radiation Oncology 29 (2021) 1–7

Contents lists available at ScienceDirect

Clinical and Translational Radiation Oncology

journal homepage: www.elsevier.com/locate/ctro

Original Research Article

The technical design and concept of a PET/CT linac for biology-guided radiotherapy

Oluwaseyi M. Oderinde *, Shervin M. Shirvani, Peter D. Olcott, Gopinath Kuduvalli, Samuel Mazin, David Larkin

RefleXion Medical, Inc, Hayward, CA, USA

ARTICLE INFO

Article history:
Received 15 December 2020
Revised 30 March 2021
Accepted 7 April 2021
Available online 17 April 2021

Keywords:
BgRT
Real-time tracking
Biological signature
Positron emission tomography
Sub-second latency

ABSTRACT

This is a summary of the design and concept of the RefleXion X1, a system for biology-guided radiotherapy (BgRT). This system is a multi-modal tomography (PET, fan-beam kVCT, and MVD) treatment machine that utilizes imaging and therapy planes for optimized beam delivery of IMRT, SBRT, SRS, and BgRT radiotherapy regimens. For BgRT delivery specifically, annihilation photons emanating outward from a PET-avid tumor are used to guide the delivery of beamlets of radiation to the tumor at sub-second latency. With the integration of PET detectors, rapid beam-station delivery, real-time tracking, and high-frequency multi-leaf collimation, the BgRT system has the potential to deliver a highly conformal treatment to malignant lesions while minimizing dose to surrounding healthy tissues. Furthermore, the potential use of a single radiotracer injection to guide radiotherapy to multiple targets opens avenues for debulking in advanced and metastatic disease states.

1. Introduction

Optimized radiation treatment aims to accurately irradiate tumoral tissues while sparing the surrounding normal tissue [1,2]. This goal must address and overcome the challenges of intra-fractional and inter-fractional changes in tumor location [3]. With the advent of hypo-fractionated treatment, image-guided radiotherapy (IGRT) has become standard for enabling more accurate and repeatable treatments in several indications [4]. Nonetheless, conventional IGRT typically relies on an image of a tumor that precedes radiotherapy delivery and does not adjust to changes in tumor position that may occur as treatment is ongoing. Several modalities such as ultrasound, stereoscopic X-ray, implanted radiofrequency-emitting fiducials, and on-board magnetic resonance imaging (MRI) have been considered for providing more "real-time" tumor tracking during radiation delivery [5–7]. However, each of these methods is limited by complex workflows or uncertainties in tumor position that require additional compensation, such as gating delivery to a single phase of respiration.

The RefleXion™ X1 biology-guided radiotherapy system (RefleXion Medical Inc, Hayward, CA) seeks to overcome these hurdles by enabling a tumor to communicate its present position directly to a linear accelerator. This technology combines dual imaging technologies (CT and PET) with a slice therapy linear accelerator [8]. Fundamentally, the system functions by utilizing kVCT imaging for initial patient setup and then PET detection of outgoing tumor emissions to detect the location of a tumor and respond with beamlets of radiotherapy with sub-second latency. This direct feedback loop between the lesion itself and treatment machine allows the system to accurately guide and conform radiation beamlets to the tumor as the tumor is moving during ongoing treatment, resulting in a tracked dose distribution characterized by high dose falloff and less dose to normal tissues than conventional radiotherapeutic approaches.

This improvement in the therapeutic ratio stems from two features. Firstly, the tumor's emitted PET profile or biological signature acts as a fiducial, which increases the confidence in lesion localization during treatment [9,10]. Therefore, the clinical team can reduce the positional margins in the treatment plan that account for setup errors and patient drifts. Secondly, the BgRT tomographic delivery algorithm does not require surrogate motion sensors, predictive motion models, or breath-hold coaching techniques. This simplification of workflow in combination with a sub-second (350–400 ms) latency means that the BgRT system can manage motion in a wide range of indications throughout the body. In turn, the clinician can avoid approaches in which

* Corresponding author at: RefleXion Medical, Inc, 25841 Industrial Blvd, #275 Hayward, CA 94545, USA.
E-mail address: ooderinde@reflexion.com (O.M. Oderinde).

https://doi.org/10.1016/j.ctro.2021.04.003
2405-6308/

the entire motion envelope (also termed the internal target volume) and all normal tissues within it must be ablated to ensure target coverage.

Notably, implied in BgRT is the potential to use a single radiotracer injection to efficiently manage motion across multiple targets in a single patient. This application may open avenues for investigating the role of radiotherapy for debulking disease in patients with metastatic cancer who are currently not candidates for radiotherapy in light of the logistical limitations of present-day technology. This work presents the design and concept of a BgRT system.

2. Technical design and chief hardware components

The X1 is currently FDA-cleared for delivering intensity-modulated radiotherapy (IMRT), stereotactic radiosurgery (SRS), and stereotactic body radiotherapy (SBRT). It is designed to eventually support biology-guided radiotherapy (BgRT). Fig. 1 shows some of the main subcomponents of the X1. The system is a fast-rotating slip-ring gantry system with a bore diameter of 85 cm that consists of two planes on the same 60 RPM gantry. These two planes are dedicated to kVCT imaging and PET-guided therapy, respectively. The kVCT imaging axial plane is parallel and anterior to the PET-guided therapy central plane with a separation of 38.6 cm axially (IEC-Y axis). In the PET-guided therapy plane, a linear accelerator (linac) head is placed between two 90° PET detector arcs. A mega-voltage detector (MVD) array is fixed directly opposite the linac head. These components are described in more detail below.

2.1. Compact linear accelerator

The linac produces a flattening filter free (FFF) photon beam of 6 MV with a nominal dose-rate of 850 cGy/min. It is equipped with a tungsten alloy target, fixed primary collimator, and an adjustable binary multi-leaf collimator (MLC) of 64 leaves for beamlet definition at a source-to-axis distance of 85 cm. The low-leakage tungsten MLC with a leaf thickness of 11 cm has an ultra-fast transition time to reduce the latency between PET data acquisition and radiation beam delivery. This design, which required development of a novel pneumatic spring-based mechanism for leaf transitions, facilitates the rapid movement of collimator leaves such that the collimator is capable of switching leaves between open and closed states in about 7 ms. The binary MLC is sandwiched between a split-jaw, the upper jaw having a thickness of 55 mm and the lower jaw having a thickness of 60 mm along the IEC Z-axis. The aperture of the split-jaws can be adjusted to define a slice having a width of 1 or 2 cm. Furthermore, the split-jaw design improves the penumbra in the IEC-Y slice direction. The nominal beam treatment area is 40×1 cm^2 or 40×2 cm^2. However, the reference calibration field size area is set at 10×2 cm^2.

2.2. Positron emission tomography imaging system

The PET detector arcs are integral to BgRT, which uses PET emissions from the tumor to rapidly deliver tracked beamlets of radiation. These arcs are comprised of 64 scintillation multi-pixel counter (MPPC) modules. The PET scintillators have side shieldings, which consist of lead septa ~2 cm thick for reducing the patient scattered radiation that can cause an afterglow effect in the scintillator crystal. The BgRT workflow uses these PET detectors at three different timepoints: (1) An imaging-only session to collect PET data from the patient for use in treatment planning (acquisition time ~40 s per 2.1 mm of treatment extent), (2) a PET pre-scan session immediately prior to radiation delivery to evaluate whether the PET radiotracer avidity of the tumor(s) in the treatment plan are sufficiently consistent with the prior imaging-only session to proceed with delivery (acquisition time ~10 s per 2.1 mm of treatment extent), and (3) during BgRT delivery to actively guide the therapeutic beam. Of note, scattered radiation from the 6MV linac pulse may interact with the scintillation crystals of the PET detector arcs. These scintillation events can generate false coincidence events within 300 μs of the linac pulse. To avoid the false detection of a coincidence event, the PET scanner is gated with a blanking interval lasting approximately 300 μs immediately after the linac pulse, as shown in Fig. 2.

2.3. Kilovoltage computed tomography imaging system

The 16-slice kVCT imaging system is mounted at the gantry entrance of the BgRT system. It acquires 3D CT fan-beam images for localizing and aligning the patient for treatment delivery, just

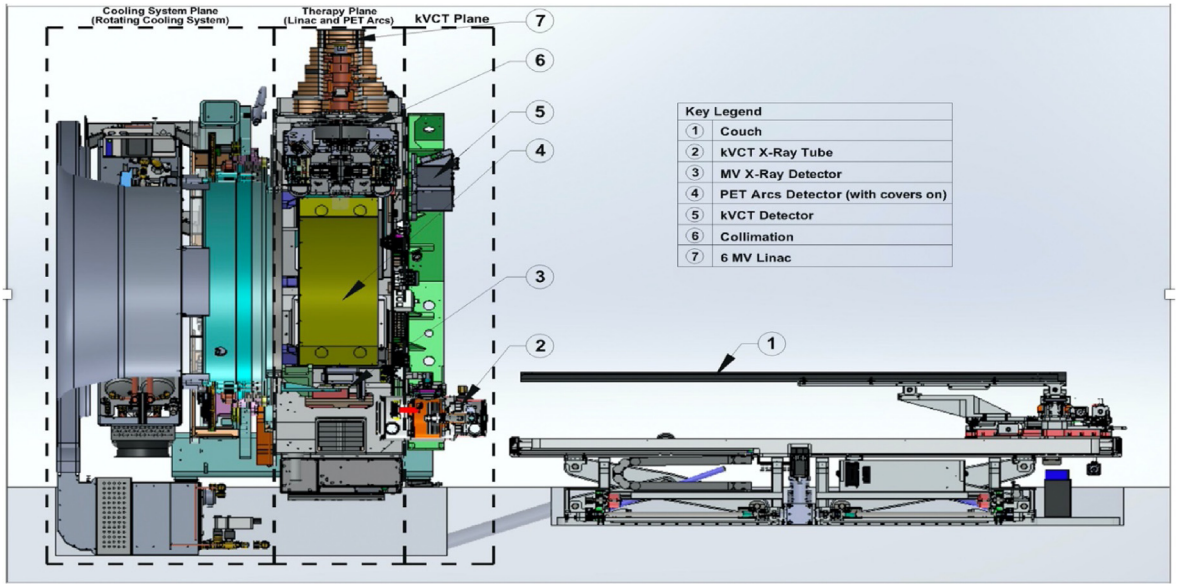

Fig. 1. An overview of the BgRT system showing some of the major subcomponents.

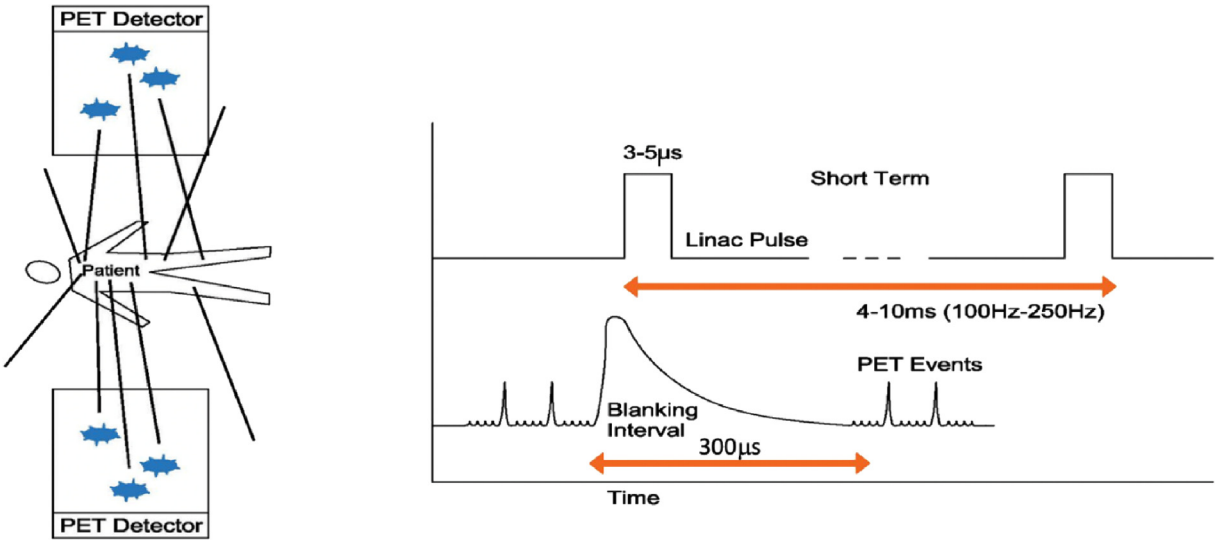

Fig. 2. The linac produces high energy photons over a concise 5-μs time interval.

as in conventional cone-beam CT (CBCT) [11,12]. It has a source-to-detector distance of 113.3 cm and source to isocenter distance of 64.3 cm for 2 cm axial coverage and 50 cm transverse field of view. The system has a bowtie filter and two-level collimators to attenuate beam exposure to peripheral extents in the IEC-X axis, and the X-ray tube has flexible movement in the IEC-X and IEC-Y directions for focal spot alignment. The system has scan modes for fast and slow helical CT with settings of up to140 kV and 300 mA and table speeds of 4.5 mm/s to 28 mm/s.

2.4. Megavoltage X-ray detector

The custom flat-panel MVD subsystem is designed to measure radiotherapy exit dosimetry and facilitate quality assurance (QA) in order to confirm proper operation of the MLC and the linac (for example: beam energy and output reproducibility). The MVD panel is made of a gadolinium oxysulfide (GOS) scintillation screen with a thin film transistor (TFT) photodiode array with an active area of 78.8 cm × 11.8 cm, which is appropriate for the largest field size on the BgRT system at a source-to-detector distance (SDD) of 136.7 cm.

2.5. Treatment couch

The BgRT system contains a robotic couch with 6 degrees of set up correction consisting of 5 physical degrees of freedom (adjustments in x-, y-, z-axes, and also pitch and yaw rotations) in addition to a slip-gantry (roll rotation) encoder offset for the 6th degree. Radiation can be delivered using single pass (for IMRT) or multi-pass (for SBRT and BgRT) motions, with a "pass" defined as the movement of the treatment couch in the IEC-Y direction during treatment delivery such that a target volume passes through the treatment plane once. For multi-pass couch motions, the patient's treatment extent typically passes through the therapy plane four times (back and forth process) in the IEC-Y direction. During each pass, the couch pauses at a set of discrete positions separated by 2.1 mm called beam stations, as shown in Fig. 3. Of note, the use of discrete beam stations is distinct from other gantry-based systems which utilize constant couch motion through the treatment plane in the IEC-Y direction. This characteristic provides better beam modulation along IEC-Y and therefore more flexibility during treatment planning.

The purpose of the multi-pass couch motion technique is to reduce dose artifacts caused by the interplay effect between MLC and tumor motion. In BgRT delivery, the number of gantry rotations per beam station is precomputed during treatment planning and identical across all beam stations. In sequential order, the treatment couch automatically moves from one beam station to another until the treatment plan is fully delivered.

3. Conceptual underpinning and treatment planning for biology-guided radiotherapy

3.1. Overview of BgRT treatment planning

BgRT delivers a radiotherapy beam based on PET data emanating outward from a tumor. Essentially, the radiotracer uptake converts the tumor itself into a biological fiducial for localization and delivery of a tracked dose. Understanding the features of active delivery help frame the BgRT algorithm and the output of the treatment planning process.

During active treatment, rapidly-acquired limited time sampled (LTS) PET images guide beamlets of radiation according to predefined coverage goals. Treatment is delivered across a sequence of beam stations. For every beam station, delivery is further divided across multiple firing positions (FPs)/couch angles subgroups. At the commencement of treatment, the first 20 FPs (25 ms/FP) are used to collect the initial PET data as shown in Fig. 4. Afterward, there is a reconstruction and calculation of the MLC sequence over 100 ms in 10 ms interval, while the beam is continuously and simultaneously delivered in parallel with the PET image acquisition. The LTS image is refreshed every 100 ms using the last 500 ms of information, as shown in Fig. 4. This refreshed LTS is subsequently used in a firing calculation to determine machine instructions for the partial fluences, which are delivered over the next 10 firing positions that the linac head passes through. This cycle is repeated in such a way that the aggregate of partial fluences delivers the intended dose to the tumor target and meets the specified limits for surrounding tissues. Furthermore, this process must be robust to some degree of variation in PET signal or tumor motion that is expected to occur from fraction to fraction. In summary, the gantry is continuously rotating while the couch is stopped at each beam station and the LTS image acquisition and treatment delivery occur simultaneously.

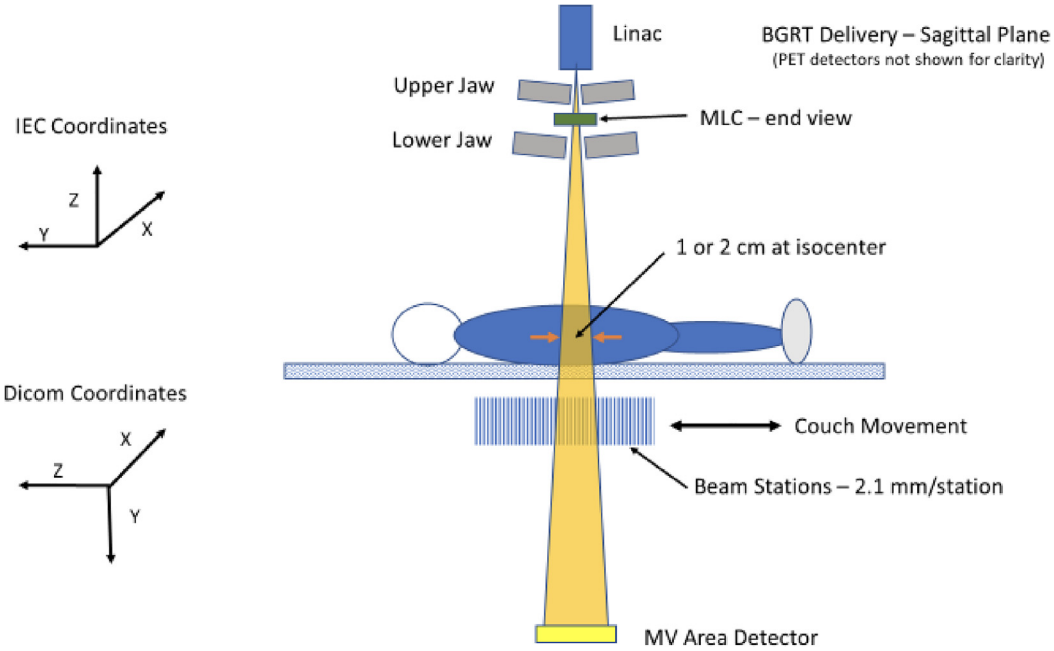

Fig. 3. Depiction of the couch movement during delivery.

In order to retain all of these qualities during active delivery, the BgRT treatment planning algorithm is necessarily different than existing radiotherapy planning algorithms, while building upon optimization principles of IMRT, SRS, and SBRT. Initially, CT simulation and CT-defined RT structures are imported into the BgRT treatment planning system (TPS) to initiate the planning process. Next, a BgRT imaging-only session is performed to acquire PET emission data from the region of the body containing the target tumor. The BgRT TPS algorithm then generates a plan that calculates a fluence map using the planning PET images to achieve the prescribed dose objectives. These steps are described in more detail below.

3.2. Novel contouring elements: BgM and BTZ

The International Commission on Radiation Units and Measurements Reports 50, 62, 83 and 91 [13–16] described a schema for radiotherapy treatment volumes that incorporate safety margins that account for uncertainties in tumor extent, tumor motion, and patient setup. To that end, these reports defined a gross tumor volume (GTV), a clinical target volume (CTV) that accounts for microscopic disease, and a planning target volume (PTV) that compensates for uncertainties in planning or treatment delivery. An internal target volume (ITV) has also been defined to capture the range of internal motion for a mobile tumor. The conventional aim for treatment planning is to achieve an optimal treatment delivery to the CTV by targeting the PTV (or ITV) while limiting exposure to nearby organs at risk (OAR).

The BgRT TPS adds two new concepts to this schema. First, a biology-guidance margin (BGM) is used to define an expansion from a GTV/CTV to PTV that accounts for localization errors intrinsic to BgRT, such as the residual latency between PET emission collection and beamlet delivery. Importantly, because BgRT results in a tracked dose distribution, the PTV can be defined with an expansion of the GTV/CTV at a single timepoint. This has potential dosimetric advantages over an ITV approach that requires adding a margin to the aggregation of the tumor's position across all phases of respiration in order to form the final treatment volume (Fig. 5).

The second novel concept is the introduction of a new region, termed the biology-tracking zone (BTZ). The BTZ encompasses the motion extent of the target with an additional margin to capture biology-guidance margin as well as patient set-up error, as shown in Fig. 5. Benchtop testing suggests that the total margin required is 5 mm. Similar to an ITV, the motion extent for the BTZ is delineated from a 4D-CT image set that is acquired during the CT simulation, which shows the position of the target tumor at each phase of the respiratory cycle. However, unlike an ITV, the BTZ does not constitute a treatment volume. Instead, it acts to limit the region from which PET emissions are gathered to guide radiotherapy; as such, it prevents emissions from non-target, PET-avid structures from influencing treatment delivery.

3.3. BgRT plan optimization

Like other radiotherapy inverse-planning algorithms, the goal of the BgRT optimization algorithm is to minimize a cost function whose inputs are physician-defined target coverage goals and OAR constraints. A traditional IMRT algorithm uses a cost function numerical score to identify a fluence map, *F*, that generates an optimal dose distribution in the patient's anatomy that meets dosimetric objectives. BgRT likewise uses an inverse-planning optimization algorithm to achieve a global minimum cost function through several iterations with an automated stopping criterion. However, the essential difference for BgRT is that the fluence map itself is defined by an operator (P) acting on a matrix of tumor PET projections (X) circumferentially arranged around the patient:

$$F = P \cdot X$$

Data that informs the PET projection matrix, X, is obtained at a PET imaging-only session on the X1. Because the tumor PET projection is a fixed quantity, the optimization algorithm uses the cost function to find the optimal operator, P, which is termed the "firing filter". This concept is schematized in Fig. 6: The simulation CT images, RT structures, PET planning images, and dose objectives are all inputs to generating the optimal firing matrix using the cost function optimization process.

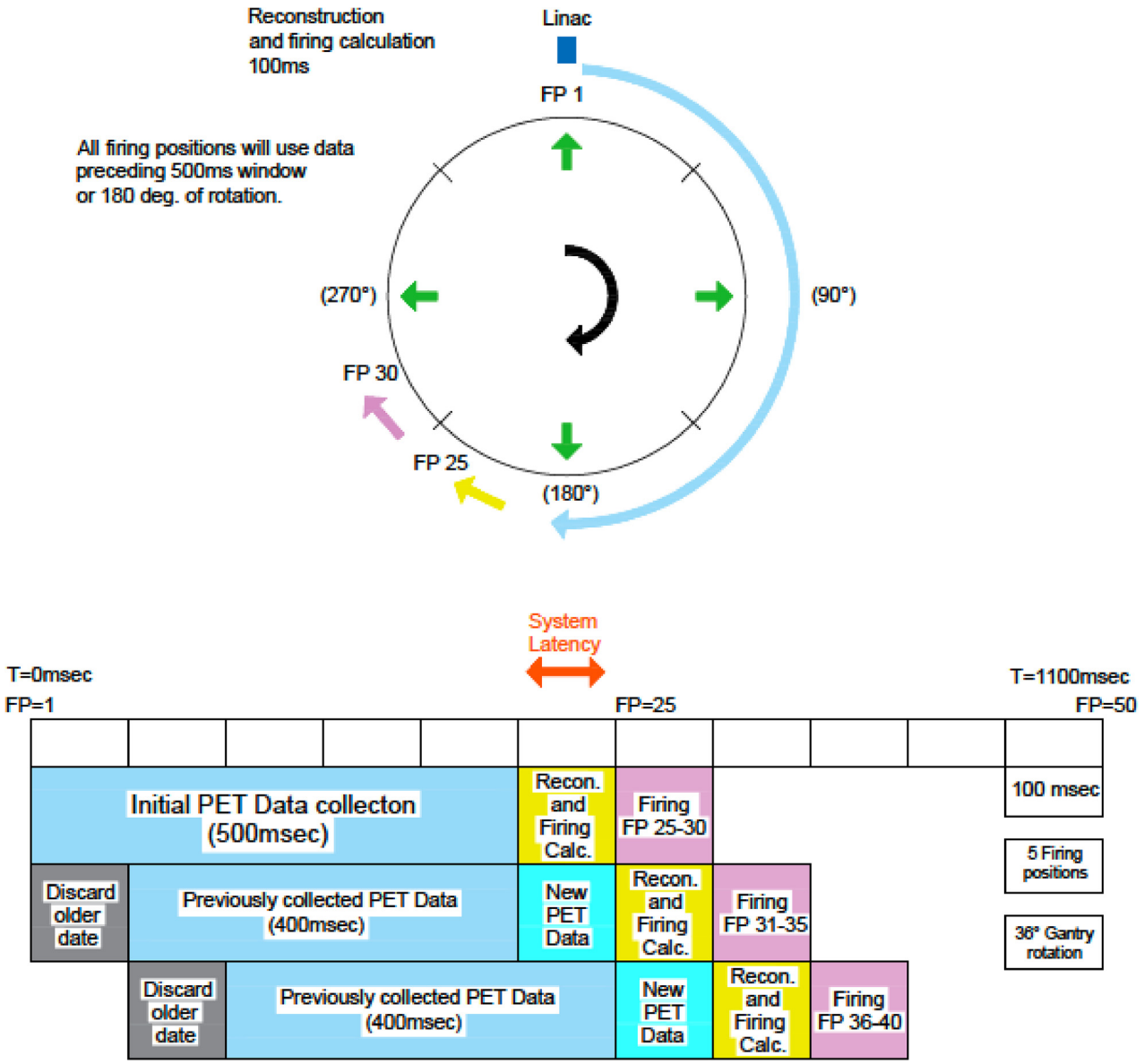

Fig. 4. System latency in the BgRT radiotherapy system.

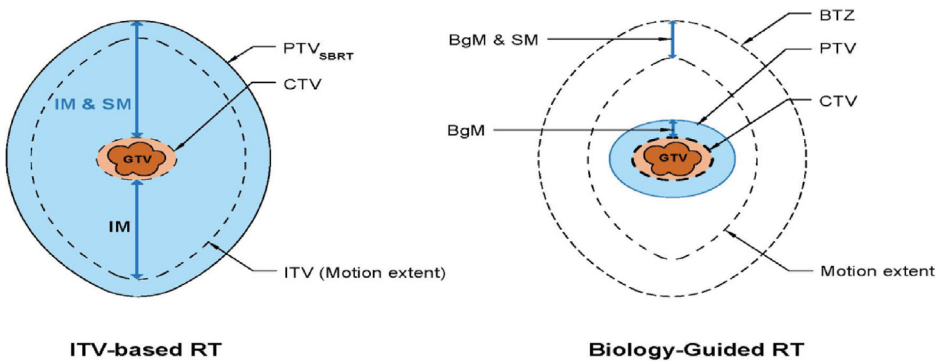

Fig. 5. Comparison of volumes used for ITV-based RT, such as SBRT (left) and BgRT (right). IM-internal margin, SM – setup margin, GTV – gross tumor volume, CTV – clinical target volume, ITV – internal target volume, PTV – planning target volume, BgM – biology – guidance margin, and BTZ-biology tracking zone.

Importantly, once the firing filter is created, the principle of superposition allows for it to be applied to limited-time sample PET images, x_i, to generate partial fluences such that the sum of partial fluences is the intended total fluence. Mathematically, this can be expressed as such:

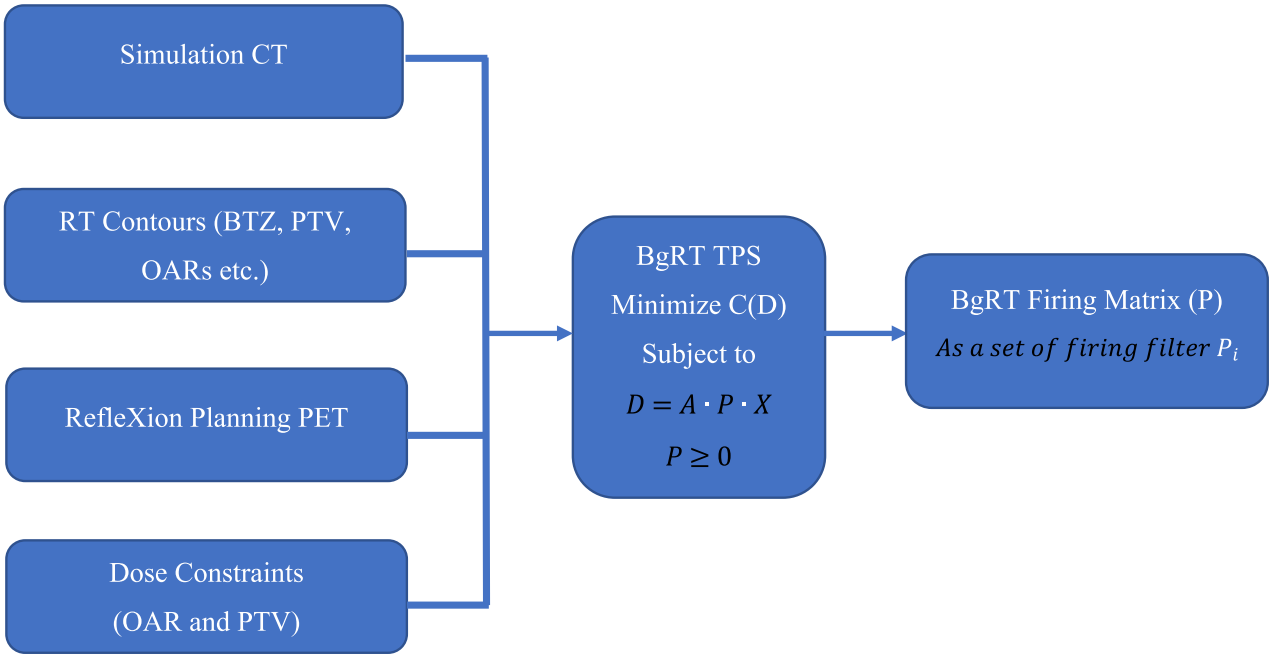

Fig. 6. BgRT plan optimization (A) overview of BgRT TPS input and output. D = Dose Distribution, C = Cost function, A = Dose calculation matrix, P = Firing Matrix, the matrix-vector product P·X is assumed to be evaluated with 3D volume X linearized into a vector.

$$F = P \cdot X = P \cdot \sum_{i}^{n} x_i = \sum_{i}^{n} P \cdot x_i$$

This principle underpins the "real-time" nature of biology-guided radiotherapy because it allows radiotherapy beamlets to be directed in response to rapidly collected packets of PET emissions. This feature avoids the fundamental deficit of typical image-guided forms of radiotherapy where a full image has to be formed prior to radiation delivery. Since it takes a longer time to generating a full image, the information contained in the full image is stale to some degree by the time the radiotherapy beam is activated.

3.4. Bounded dose-volume histogram (bDVH)

The dose distribution in the patient is calculated using the collapsed-cone convolution (CCCS) algorithm with recursive formulation [17]. The BgRT TPS accounts for the cumulative-cumulative kernel (tabulated kernel) approach and different voxel size effects [18]. An additional feature is that the TPS models scenarios where either the PET signal over background or tumor position changes between the PET imaging-only session and the day of BgRT delivery. Plans that account for tumor-to-background signal variations of ±25% relative to baseline and tumor shifts of 5 mm in all 3 directions are calculated during treatment planning. The BgRT TPS simulates multiple dose-volume histograms (DVHs) using these possible permutations and then collectively visualizes the possibilities in a bounded DVH (bDVH) where the DVH line for each volume and OAR is surrounded by confidence intervals representing the different variations. As such, the bDVH shows the potential best case and worst case dosimetric outcomes for a given treatment plan and delivery so that the plan's merits can be comprehensively evaluated.

4. Clinical workflow for the BgRT system

To select a patient for BgRT, an optional staging PET/CT may be used to determine whether the target lesion is sufficiently radiotracer-avid. If the target lesion takes up the radiotracer, then the full workflow can be initiated. Standard radiotherapy workflow includes the steps of prescription, simulation, treatment planning, and treatment delivery [19,20]. As illustrated in Fig. 7, the BgRT clinical workflow adds steps to the standard radiotherapy workflow so that dynamic PET targeting can be incorporated.

The additional steps are the BgRT imaging-only session and the PET pre-scan. The imaging-only session serves to assess formal candidacy for BgRT (i.e., sufficient radiotracer activity as observed by the intrinsic RefleXion PET subsystem). As described above, this step also provides the PET data that underpins the treatment planning algorithm as described above.

After the BgRT plan is approved, the patient undergoes a PET pre-scan immediately prior to actual delivery. This step generates a predicted dose distribution from the tumor PET signal and motion pattern that day. The system checks to ensure that the predicted DVH from the pre-scan data fits within the bounds of the bDVH approved at planning. The pre-scan image can be reviewed by the clinician to confirm that the target is within the BTZ on the day of the treatment. Finally, if all criteria are satisfied, BgRT delivery can commence. If the criteria are not satisfied, the clinician can choose to abort and reschedule treatment or instead use a fall-back CT-guided plan generated in parallel with the BgRT plan. These steps are schematized in Fig. 7. This process is repeated for each fraction until treatment is complete.

Of note, a radiotracer injection can be used to "fiducialize" every site of gross disease which takes up the radiotracer. Therefore, by acting as a unified motion management solution across different anatomic locations, the BgRT workflow holds promise as a platform for efficiently ablating multiple malignant lesions in a metastatic patient.

5. Conclusion

Biology-guided radiotherapy has the potential to improve upon current radiation methods by reducing treatment margins around targets and better compensating for motion. To translate this innovative concept into the real-world practice, unique and novel ele-

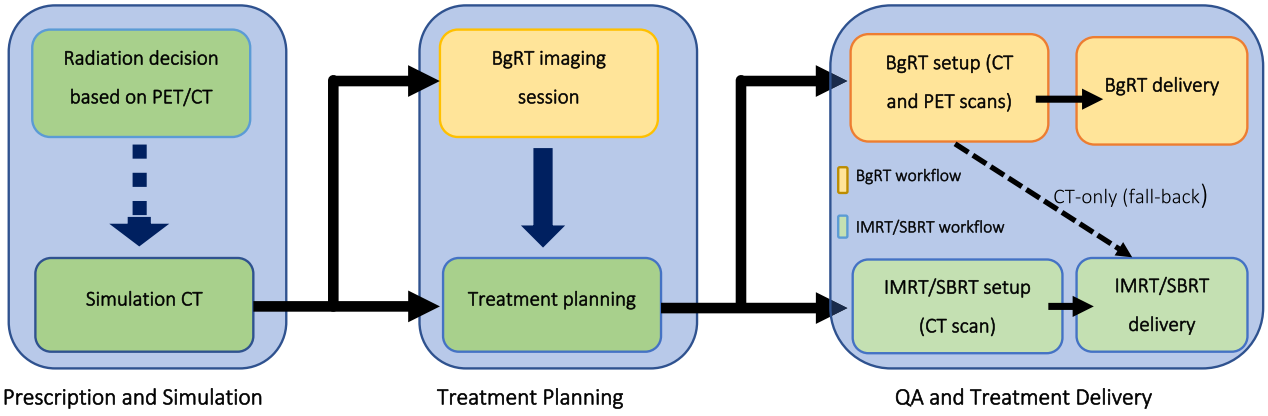

Fig. 7. Proposed clinical workflow of BgRT system.

ments for hardware, treatment planning, and workflow were developed, engineered, and integrated into the design of the RefleXion X1. Because radiotracer injections can result in uptake at multiple tumor sites, this platform may provide a vehicle for efficient radio-ablation of multiple lesions in the same treatment session for patients with clinically-evident metastatic disease.

Declaration of Competing Interest

The authors declare the following financial interests/personal relationships which may be considered as potential competing interests: The authors are RefleXion Medical, Inc. employees.

Acknowledgements

The authors wish to thank Judy Bartlett-Roberto and Ann Yang for editing this report and Raquel Pires for assisting with the pictorial design of the figures (employees RefleXion Medical, Inc.).

References

[1] Alber M, Nüsslin F. An objective function for radiation treatment optimization based on local biological measures. Phys Med Biol 1999;44(2):479–93. https://doi.org/10.1088/0031-9155/44/2/014.
[2] Brahme A. Development of radiation therapy optimization. Acta Oncol 2000;39(5):579–95. https://doi.org/10.1080/028418600750013267.
[3] Michalski A, Atyeo J, Cox J, Rinks M. Inter- and intra-fraction motion during radiation therapy to the whole breast in the supine position: a systematic review. J Med Imaging Radiat Oncol 2012;56(5):499–509. https://doi.org/10.1111/j.1754-9485.2012.02434.x.
[4] Chang JY, Dong L, Liu H, Starkschall G, Balter P, Mohan R, et al. Image-guided radiation therapy for non-small cell lung cancer. J Thorac Oncol 2008;3(2):177–86. https://doi.org/10.1097/JTO.0b013e3181622bdd.
[5] Cerviño LI, Du J, Jiang SB. MRI-guided tumor tracking in lung cancer radiotherapy. Phys Med Biol 2011;56(13):3773–85. https://doi.org/10.1088/0031-9155/56/13/003.
[6] Zhong Y, Stephans K, Qi P, Yu N, Wong J, Xia P. Assessing feasibility of real-time ultrasound monitoring in stereotactic body radiotherapy of liver tumors. Technol Cancer Res Treat 2013;12(3):243–50. https://doi.org/10.7785/tcrt.2012.500323.
[7] Ting L-L, Chuang H-C, Liao A-H, Kuo C-C, Yu H-W, Tsai H-C, et al. Tumor motion tracking based on a four-dimensional computed tomography respiratory motion model driven by an ultrasound tracking technique. Quant Imaging Med Surg 2020;10(1):26–39. https://doi.org/10.21037/qims.2019.09.02.
[8] Shirvani SM, Huntzinger CJ, Melcher T, Olcott PD, Voronenko Y, Bartlett-Roberto J, et al. Biology-guided radiotherapy: redefining the role of radiotherapy in metastatic cancer. Br J Radiol 2020;94(1117):20200873. https://doi.org/10.1259/bjr.20200873.
[9] Ling CC, Humm J, Larson S, Amols H, Fuks Z, Leibel S, et al. Towards multidimensional radiotherapy (MD-CRT): biological imaging and biological conformality. Int J Radiat Oncol Biol Phys 2000;47(3):551–60. https://doi.org/10.1016/s0360-3016(00)00467-3.
[10] Yang J, Yamamoto T, Mazin SR, Graves EE, Keall PJ. The potential of positron emission tomography for intratreatment dynamic lung tumor tracking: a phantom study. Med Phys 2014;41(2):021718. https://doi.org/10.1118/1.4861816.
[11] Yeung AR, Li JG, Shi W, Newlin HE, Chvetov A, Liu C, et al. Tumor localization using cone-beam CT reduces setup margins in conventionally fractionated radiotherapy for lung tumors. Int J Radiat Oncol Biol Phys 2009;74(4):1100–7. https://doi.org/10.1016/j.ijrobp.2008.09.048.
[12] Wang Z, Wu QJ, Marks LB, Larrier N, Yin F-F. Cone-beam CT localization of internal target volumes for stereotactic body radiotherapy of lung lesions. Int J Radiat Oncol Biol Phys 2007;69(5):1618–24. https://doi.org/10.1016/j.ijrobp.2007.08.030.
[13] Jones D. Prescribing, recording and reporting photon beam therapy ICRU report 50. Med Phys 1994;21(6):833–4. https://doi.org/10.1118/1.597396.
[14] Landberg T, Chavaudra J, DobbsPrescribing J. Recording and reporting photon beam therapy (supplement to ICRU report 50). In: 62. Bethesda, USA: ICRU Report 62; 1999. https://doi.org/10.1093/jicru_os32.1.48.
[15] DeLuca P, Jones D, Gahbauer R, Whitmore G, Wambersie A. Prescribing, recording and reporting intensity-modulated photon-beam therapy (IMRT) Report 83. Bethesda, USA: ICRU Report 83; 2010.
[16] Seuntjens J et al. Prescribing, recording, and reporting of stereotatic treatments with small photon beams; 2014.
[17] Ahnesjö A. Collapsed cone convolution of radiant energy for photon dose calculation in heterogeneous media. Med Phys 1989;16(4):577–92. https://doi.org/10.1118/1.596360.
[18] Lu W, Olivera GH, Chen M-L, Reckwerdt PJ, Mackie TR. Accurate convolution/superposition for multi-resolution dose calculation using cumulative tabulated kernels. Phys Med Biol 2005;50(4):655–80. https://doi.org/10.1088/0031-9155/50/4/007.
[19] Manyam B, Yu N, Meier T, Suh J, Chao S. A review of strategies for optimizing workflow, quality improvement, and patient safety within radiation oncology departments. Appl Rad Oncol 2018;7(4):8–12.
[20] McShan DL. Workflow and clinical decision support for radiation oncology. In Effic. decis. support syst. – pract. chall. biomed. relat. Domain; 2011.